The Cryosphere Discuss., https://doi.org/10.5194/tc-2017-247
Manuscript under review for journal The Cryosphere
Discussion started: 1 December 2017

The Cryosphere Discussions
Open Access
EGU

Thin sea ice in the Arctic: comparing L-band radiometry retrievals with an ocean reanalysis

Steffen Tietsche[1], Magdalena Alonso-Balmaseda[1], Patricia Rosnay[1], Hao Zuo[1], Xiangshan Tian-Kunze[2], and Lars Kaleschke[2]

[1]European Centre for Medium-Range Weather Forecasts
[2]Institute of Oceanography, University of Hamburg

Correspondence to: S. Tietsche (s.tietsche@ecmwf.int)

Abstract. L-band radiance measurements such as these from the SMOS satellite can be used to distinguish thin from thick ice under cold surface conditions. However, uncertainties can be large due to assumptions in the forward model that converts brightness temperatures into ice thickness, and due to uncertainties in ancillary fields which need to be independently modelled or observed. It is therefore advisable to perform a critical assessment with independent observational and model data, before using these data for model validation or data assimilation. Here, we discuss version 3.1 of the University of Hamburg L3C SMOS sea-ice thickness data set (SMOS-SIT) from autumn 2010 to spring 2017, and compare it to the results of the global ocean-sea ice analysis ORAS5. It is concluded that SMOS-SIT provides valuable and unique information on thin sea ice during winter, both in terms of the seasonal evolution and interannual variability. Overall, there is a promising match between SMOS-SIT and ORAS5 early in the freezing season (October-December), while later in winter, sea ice is consistently modelled thicker than observed. This seems to be mostly due to deficiencies of the model to simulate polynyas and fracture zones. However, there are regions where biases in the observational data seem to play a role, as comparison to independent observational data suggests. Both the reanalysis and the observations are provided with uncertainty estimates. While the reanalysis uncertainty estimates for the thickness of thin sea ice are probably too small and do not include structural uncertainty of the simulation, these of SMOS-SIT are often large, and do not seem to adequately characterise the complex uncertainties of the retrieval model. Therefore, careful and manual assessment of the data when using it for model evaluation and data assimilation is advisable. Interannual variability and trends of the large-scale distribution of thin sea ice are in good agreement between SMOS-SIT and ORAS5. In summary, SMOS-SIT presents a unique source of information about thin sea ice in the winter-time Arctic, and its use in sea ice modelling, assimilation and forecasting application is nascent and promising.

1 Introduction

Sea ice has been regularly observed by satellites since the late 1970s. The most useful observations for use in large-scale weather and climate models come from passive microwave radiance in the range between 6 and 90 GHz, with a continuous daily pan-Arctic coverage a resolution of 50km or better. However, because of the very small penetration depth into ice at

The Cryosphere Discuss., https://doi.org/10.5194/tc-2017-247
Manuscript under review for journal The Cryosphere
Discussion started: 1 December 2017

these frequencies, these observations only provide information about the fraction of an area covered by sea ice, not about its thickness.

Considering the importance of sea-ice thickness for atmosphere-ocean for surface heat fluxes, and for predicting the further evolution of the sea-ice cover, information about it is indispensable. Substantial heat conduction through thin sea ice occurs in winter, when the temperature contrast between the cold surface atmosphere and the relatively warm ocean water becomes large. Approximate calculations show that surface heat fluxes resulting from heat conduction through thin sea ice can easily reach $100\,\mathrm{Wm}^{-2}$. Predicting the evolution of the sea-ice cover days to months ahead also crucially depends on the sea-ice thickness: thin ice will evolve much more quickly than thick ice because it is more susceptible to dispersion or compression by winds, and by allowing larger surface heat fluxes it can lose or gain mass much faster than thick ice.

The thickness of sea ice is much harder to derive from satellite observations, and each of the existing methods has its own strong limitations. Infrared emission measurements of the ice surface temperature (Wang et al., 2010; Yu and Rothrock, 1996; Mäkynen et al., 2013) only work for very thin ice without snow cover, and can only be used for cloud-free conditions. Laser and radar altimetry (Kwok and Cunningham, 2008; Laxon et al., 2013; Ricker et al., 2014) suffers from high measurement noise and narrow foot-prints, and has larger errors for thicknesses below 0.5 m. The third method, L-band microwave radiance measurements (Kaleschke et al., 2012; Tian-Kunze et al., 2014; Mecklenburg et al., 2016), allows daily pan-Arctic coverage for ice thickness of up to 1m with about 30km spatial resolution. It requires however a complex radiative transfer model – calculated emissivities might be sensitive to assumptions and ancillary fields used.

This study investigates the properties of a level-3 sea ice thickness product provided by the University of Hamburg (SMOS-SIT), and compares it with the global ocean-sea ice reanalysis ORAS5 produced by the European Centre for Medium-Range Weather Forecasts (ECMWF). Non-trivial model-observation departures are reported, which change with region, time of the year, and thickness range considered. Routine monitoring of the departures has been implemented at ECMWF, and this investigation is a step towards eventual assimilation of the data, although successful assimilation will require further improvements in the model, observation retrievals, and data assimilation methods.

2 Model and data

2.1 SMOS-SIT sea ice thickness product

Thin sea ice thickness (nominal cut-off at 1.5 m) has been retrieved at the University of Hamburg from L-band brightness temperatures measured by the MIRAS radiometer on board of SMOS. The retrieval algorithm consists of a thermodynamic sea ice model and a one-ice-layer radiative transfer model (Kaleschke et al., 2012; Tian-Kunze et al., 2014). The resulting plane layer thickness is multiplied by a correction factor assuming a log-normal thickness distribution (Tian-Kunze et al., 2014). The algorithm has been used for the operational production of a SMOS-based sea ice thickness data set in polar-stereographic projection in 12.5 km grid resolution from 2010 on (http://icdc.cen.uni-hamburg.de/1/daten/cryosphere/l3c-smos-sit.html) (Tian-Kunze et al., 2014). In this study we use the most up-to-date version (v3.1, based on v620 L1C brightness temperatures), which has been produced operationally since October 2016. The v3.1 data for the previous winter seasons had been reprocessed using

the same algorithm. The previous versions of the algorithm have been described in Kaleschke et al. (2012); Tian-Kunze et al. (2014); Kaleschke et al. (2016), who also provide comparison to EM-bird measurements, infrared-derived, and modelled sea ice thickness.

Brightness temperature used in the algorithm is the daily mean intensity, which is the average of horizontal and vertical polarization. Over sea ice, the intensity is almost independent of incidence angle. The average over the incidence angles 0-40° is taken, in order to reduce the brightness temperature uncertainty to about 0.5 K. In the beginning two years of SMOS operation, the signals were strongly influenced by Radio Frequency Interference (RFI). In the algorithms prior to v3.1, RFI contaminated snapshots have been discarded using a threshold value of 300 K, applied either to horizontal or vertical polarization. However, in v3.1 the new quality flags given in the v620 L1C data have been implemented to identify the data contaminated not only by RFI but also by sun, or by geometric effects.

The retrieval method needs additional auxiliary data as boundary conditions for the thermodynamic as well as the radiation model: bulk ice temperature is estimated from surface air temperature extracted from the JRA-55 atmospheric reanalysis (ONOGI et al., 2007). Bulk sea-ice salinity is calculated with the methods described in Tian-Kunze et al. (2014) based on a weekly climatology of sea surface salinity from a simulation with the MIT General Circulation Model (Marshall et al., 1997) covering the years 2002-2009. Brightness temperatures over sea ice depend on the dielectric properties of the ice layer, which vary with ice temperature and ice salinity (Menashi et al., 1993; Kaleschke et al., 2010, 2012). For a thin ice layer, the ice temperature gradient within the ice can be assumed to be linear. The retrieval algorithm works only under cold conditions: the presence of surface melting invalidates the retrieval assumptions.

Ice thickness uncertainties are given pixel-wise each day in the data set. There are several factors that cause uncertainties in the sea ice thickness retrieval: the uncertainty of the SMOS measurements, the uncertainties in the ice temperature and ice salinity, and the assumptions made for the radiation and thermodynamic models, for example 100% ice coverage. A 100% ice coverage assumption made in the retrieval can cause underestimation of ice thickness if the condition is not met (Tian-Kunze et al., 2014). Other than in previous versions, in v3.1 we also consider the uncertainty caused by the thickness distribution function, which is estimated to be less than 10 cm.

For more detailed technical information and a discussion of the limits of SMOS-SIT please refer to the Appendices. Appendix A shows that there are some substantial differences in the SMOS-SIT data set between the current version 3.1 and the previous version 2.3. In Appendix B, the fundamental limits of retrieving sea-ice thickness from SMOS brightness temperatures are touched upon, and evidence for these limits from the data themselves is presented. Appendix C discusses unrealistic day-to-day fluctuations in retrieved sea-ice thickness, and Appendix D demonstrates that using SMOS-SIT without removing high-uncertainty data points can lead to wrong conclusions when studying year-to-year variability of thin sea ice.

2.2 ORAS5 sea-ice–ocean reanalysis

The ECMWF ocean reanalysis system 5 (ORAS5) is a state estimate of the global ocean and sea ice from 1975 to today, and is being used to provide ocean and sea ice initial conditions for operational forecasts at ECMWF (Zuo et al., 2017).

The Cryosphere Discuss., https://doi.org/10.5194/tc-2017-247
Manuscript under review for journal The Cryosphere
Discussion started: 1 December 2017

The NEMO ocean model version 3.4.1 (Madec, 2008) has been used for ORAS5 in a global configuration with a tripolar grid with a resolution of 1/4 degree at the equator. One of the poles of the grid is located on the Antarctic continent, and the other two are in Central Asia and North Canada. Horizontal resolution in northern high latitudes ranges from less than 5 km (Canadian Archipelago south of Victoria Island) to about 17 km (Bering Sea and Sea of Okhotsk). There are 75 vertical levels, with level spacing increasing from 1 m at the surface to 200 m in the deep ocean.

ORAS5 contains the dynamic-thermodynamic sea ice model LIM2 (Fichefet and Maqueda, 1997). The sea ice model is run with a viscous-plastic rheology. LIM2 has fractional ice cover, a single ice thickness category (Hibler III, 1979), and calculates vertical heat flux within the ice according to the three-layer Semtner scheme (Semtner, 1976). Snow on sea ice is modelled, but melt ponds are not.

Forcing fields for ORAS5 are derived from the atmospheric reanalysis ERA-Interim (Dee et al., 2011) until the end of 2014, and from the operational ECMWF atmospheric analysis from the beginning of 2015 on. Sea surface temperature is constrained to observations from the UK Met Office Operational Sea Surface Temperature and Sea Ice Analysis (OSTIA) by a strong restoring term. Assimilation of subsurface ocean temperature and salinity, of sea ice concentration and sea level anomalies is performed using a 3DVar-FGAT procedure (Daget et al., 2008). The length of the data assimilation window is 5 days.

Sea-ice concentration in ORAS5 is assimilated from the level-4 OSTIA product (Donlon et al., 2012). Sea-ice concentration in OSTIA is created by interpolating the OSI-SAF sea ice products (http://osisaf.met.no/p/ice) to a global regular grid with 1/20 degree resolution and filling in missing values. The sea-ice concentration assimilation is univariate with no direct impact on the floe ice thickness. However, mean ice thickness (i.e. ice volume per area) is directly impacted by the assimilation increments (see Tietsche et al. (2013) for details). There is no assimilation of sea-ice thickness observations in ORAS5.

ORAS5 consists of five ensemble members which are obtained by perturbing forcing fields according to uncertainties derived from inter-product differences, and by assimilating observations that were sampled in a slightly different way for each ensemble member.

For a full description of the immediate predecessor of ORAS5, see the documentation of ORAP5 in Zuo et al. (2015); Tietsche et al. (2015).

3 Pan-Arctic reanalysis–observation departures

SMOS-SIT data provides essential information about sea ice that is complementary to observation of sea ice concentration by higher-frequency passive microwave channels. To illustrate that, Figure 1 shows SMOS-SIT sea-ice thickness together with sea-ice concentration from the OSTIA product for a day early in the freezing season, and for a day late in the freezing season. Early in the freezing season, there are large areas of newly-formed sea ice that is thin. Figure 1a) shows that in the Beaufort and Chukchi Seas as well as the part of the Arctic Ocean adjacent to them, sea ice thickness of $0.6 - 0.7$ m dominates. In the Baffin Bay, sea ice thickness from SMOS-SIT is even thinner, at around $0.2 - 0.3$ m. All these regions exhibit high sea-ice concentration of above 90% (Figure 1b). Thus, the OSTIA sea-ice concentration product can not be used to differentiate them from the areas of older ice in the Central Arctic.

[Figure 1 about here.]

Sea-ice thickness in ORAS5 in early winter is comparable with that of SMOS-SIT (Figure 1c). However, the model tends to simulate thicker ice on average. Positive departures dominate, especially close to regions of thick ice. There are a few places in the Beaufort and the Siberian Shelf Seas with negative departures, but in most of the thin-ice areas ORAS5 simulates ice around 0.4 m thicker than retrieved by SMOS-SIT. Part of the reason for this might be the simplified representation of thin ice in ORAS5, which tends to drive modelled sea-ice thickness towards 0.6 m during the freeze-up, as can be seen in Figure 8 (see also discussion in Tietsche et al. (2014)). At the same time, ice thickness in SMOS-SIT is calculated under the assumption of 100% sea ice concentration; under the presence of only partial ice cover the SMOS-SIT ice thickness are known to be biased thin (Tian-Kunze et al., 2014).

As the freezing season progresses, the ice edge moves further south outside of the Arctic Basin, and previously formed thin ice in the Arctic Basin becomes thicker. Polynyas and fracture zones begin to form. Figure 1(d) shows large polynyas in the Kara and Laptev Seas, as well as a fracture zone covering the whole Beaufort Sea. In the Baffin Bay, sea-ice thickness derived by SMOS-SIT is mostly below 0.3 m. Again, none of these features within the ice pack are picked up by the sea-ice OSTIA concentration product, which shows homogeneously high ice concentration throughout the ice pack (Figure 1e).

The departures between ORAS5 and SMOS-SIT in late winter are large and positive throughout (Figure 1(f)), with values of 1m or more dominating. Most of this is likely due to the model being unable to simulate relevant features like the coastal polynya in the Laptev Sea, or fraction zones like the one visible in the SMOS-SIT data for the Beaufort Sea. Interestingly, in the Barents Sea there is good agreement between ORAS5 and SMOS-SIT, with a positive departure of 20 cm or less. Finally, the Baffin Bay stands out as having extensive thin ice cover in SMOS-SIT, but thick ice in ORAS5. The well-known polynya at the northern end of Baffin Bay is captured both by SMOS-SIT and ORAS5.

The previous example maps show typical conditions in early and late winter, and typical departures between ORAS5 and SMOS-SIT. For a more quantitative assessment, we calculate departures for collocated daily sea-ice thickness for each day in the early-winter period 15 October to 15 December 2015, and for each day in the late-winter period 15 February 2016 to 15 April 2016. The scatter density of the resulting set of observation-analysis pairs is shown in Figure 2.

[Figure 2 about here.]

As can be seen from Figure 2a, in early winter the agreement between SMOS-SIT and ORAS5 sea ice thickness is quite promising. The distribution is roughly along the one-to-one line. However, the overestimation of sea-ice thickness by ORAS5, which was already visually apparent from the maps in Figure 1, is confirmed. For observed sea-ice thickness between 0 and 0.3 m, ORAS5 sea-ice thickness is about 0.3 m higher. The agreement becomes better for higher observed sea-ice thickness in the range 0.5-1 m. Note that the scatter density distribution has wide tails in the ORAS5-SIT. For instance, for 0.4 m SMOS-SIT, ORAS5 SIT of up to 1.5 m exist. This is not so obvious in the scatter density, but clearly visible in the corresponding scatter plot that tends to highlight outlier data points (not shown). It is worth noting the curved shape of the scatter density distribution, which highlights the non-linear dependence of typical analysis-observation departures on the thickness range observed.

The Cryosphere Discuss., https://doi.org/10.5194/tc-2017-247
Manuscript under review for journal The Cryosphere
Discussion started: 1 December 2017

In late winter, ORAS5 has much higher sea-ice thickness than SMOS-SIT (Figure 2b). Departures between 0.5m and 1m are common throughout the SMOS-SIT thickness range of 0-1m. There is a more linear shape of the scatter density distribution – this is promising in principle, but could result from compensating errors in different regions, which would make the relationship less relevant. The scatter distribution is also much wider than for early-winter, indicating larger and more uncertain analysis-observation differences.

The larger discrepancy in later winter has several causes. Figure 1(c-f) illustrate the most obvious one: the numerical sea-ice model does not simulate polynyas and fracture zones well. But there are other causes, some of which related to the properties of SMOS-SIT data. In the following Section, we analyze the late-winter departures in more detail.

4 Regional contrasts

There is considerable regional dependence of the departures in late winter (February to April). Figure 3 shows the SMOS-SIT/ORAS5 scatter density as in Figure 2b), but for three key regions separately: the Barents and Kara Seas, the Laptev Sea, and the Baffin Bay.

For the Barents and Kara Seas (Figure 3a), the departure statistics are almost as good as for the pan-Arctic in early winter (Figure 2a). We can conclude that this region has relatively good agreement between ORAS5 and SMOS-SIT sea ice thickness throughout the winter.

In the Laptev Sea (Figure 3b), ORAS5 has no ice thickness below 1m, whereas SMOS-SIT detects a lot of ice thinner than 1m. There is hardly any correlation between ORAS5 and SMOS-SIT ice thickness, as the features of the scatter density are mostly horizontal. This behaviour is consistent with our earlier assessment that polynyas do occur frequently in the Laptev sea in late winter, and that they are detected by SMOS-SIT but not well represented in ORAS5.

Finally, Figure 3c shows the late-winter scatter density for the Baffin Bay, which again has characteristics that are very different from the other two regions. In general, ORAS5 simulates much thicker ice than retrieved by SMOS-SIT, but in contrast to the Laptev-Sea case, there is a quite well-defined concave downwards functional relationship between SMOS-SIT and ORAS5. This signals systematic rather than random sources for the departures, and would in principle allow for a successfully bias correction when mapping model equivalent to observations.

[Figure 3 about here.]

An interpretation of the results in Figure 3 needs to start from the appreciation that the regions shown have quite different physical characteristics: in the Barents and Kara Seas, sea ice is strongly affected by warm Atlantic water being advected towards and under the ice. At the same time, prevailing winds modulate the location of the ice edge by transporting the ice. Both processes are expected to be reasonably well simulated by ORAS5, because winds are prescribed as forcing, and the SST are ingested from an observational product. From the observational side, most of the calibration and validation campaigns for SMOS-SIT have been carried out in this area Kaleschke et al. (2016). Thus, the Barents and Kara Seas can be expected to be the region where the analysis-observation agreement is best.

In the Laptev Sea, ice is still relatively well observed when it comes to SMOS-SIT validation, but it is more difficult to simulate in ORAS5. Because there is no ice edge in the Laptev Sea, SST information cannot be used to constrain the ice cover. Furthermore, as clearly visible in Figure 1, extensive polynyas form there in Feb-Apr, mainly when offshore winds push back the ice from land or land-fast sea ice. These processes are not well simulated by the sea-ice model, which tends to keep a compact thick sea ice cover even in the presence of offshore winds. As a result, major departures can be expected.

Finally, in the Baffin Bay, the occurrence of thinner ice of varying thickness is modelled and observed, but the modelled ice is roughly twice as thick. There is independent information that suggests that SMOS ice thickness is biased low there (see also Landy et al. (2017)). CryoSat2 estimates (Laxon et al. (2013), http://www.cpom.ucl.ac.uk/csopr/seaice.html) indicate that between February and April, the ice in this region is typically 1.5 m thick. This is confirmed by independent expert judgement by ice chart analysts, who estimate that ice in this region and this season would typically be at least 1m thick (Nick Hughes, personal communication).

To further illustrate and consolidate the findings from Figure 3, we plot time series for two representative locations in the Laptev Sea and the Baffin Bay in Figure 4. Both show the typical behaviour of analysis-observation departures: SMOS-SIT observations and ORAS5 simulation match well early in winter, but later on the analyzed ice keeps getting thicker while SMOS-SIT thickness saturates, albeit with some strong fluctuations. We choose to present a full freezing season in the winter 2011/2012, because this allows collocation with some independent data in both locations. For the Laptev Sea (Figure 4a), there was an EM-bird overflight in April, confirming that the ice was indeed only about 0.5 m thick, which indicates the presence of new thin ice in the well-known Laptev-Sea Polynya (Tian-Kunze et al., 2014). The model is not able to simulate that. The CryoSat2 estimate for this location is around 1m averaged over March/April, halfway between ORAS5 and SMOS-SIT.

For a representative location in the Baffin Bay (Figure 4b), there is reasonable match between analysis and observations until January. After that, the sea ice in the analysis keeps growing to reach thicknesses of 1.5 - 2m in mid-April, whereas SMOS-SIT observations level off between 0.5 and 1m until mid-April. The CryoSat2 estimate for this location and averaged over March/April 2012 is 1.8m.

When judging compatibility of observational and model-based estimates of sea ice thickness, their uncertainties should be taken into account. The available uncertainty estimates are indicated in Figure 4 in the form of five perturbed ensemble members of the ORAS5 reanalysis, and in the form of lower and upper bounds of the SMOS-SIT uncertainty estimate provided with the data set. The estimated ORAS5 uncertainty is very small – well below 0.3 m most of the time. It is almost certainly too small, as it does not account for structural uncertainty in the model and data assimilation methods. By contrast, the SMOS-SIT uncertainty range is very variable, and often very large. Sometimes it covers the whole range of fathomable values; sometimes it is small, but independent evidence suggests that the truth lies far outside the uncertainty range provided. An example of the former case is the SMOS-SIT ice thickness in the Laptev Sea (Figure 4a) in February: the retrieved value is 1.2 m, but the uncertainty range goes from 0m to more than 2m. An example for the latter case is the SMOS-SIT ice thickness in the Baffin Bay in April 2012: the retrieved value is 0.5 m with an uncertainty estimate of only 0.1 m. As argued before, the true sea ice thickness was very likely much higher than that.

[Figure 4 about here.]

The Cryosphere Discuss., https://doi.org/10.5194/tc-2017-247
Manuscript under review for journal The Cryosphere
Discussion started: 1 December 2017

Given that ORAS5, CryoSat2, and expert judgement agree that sea ice in the Baffin Bay in this time of the year should be considerably thicker than SMOS-derived thicknesses, we tentatively suggest that there is a problem with the retrieval assumption of SMOS-SIT in this region. From Figures 5 (a),(e) it can be seen that the slight decrease in SMOS TB from February onwards is interpreted as a slight decrease in SIT by SMOS-SIT, in disagreement with the ORAS5 analysis. Sea ice concentration is unlikely to play a role, as it is close to 100% in both model and observations (Figure 5b). There was a considerable and varying amount of radio-frequency interference (Figure 5f), but it seems that its impact is successfully removed by the processing chain when calculating the brightness temperatures.

Surface temperature (Figure 5d) is consistently colder in ORAS5 than in SMOS-SIT. This is linked with the thicker ice which reduces conductive heat fluxes through the ice that warm the surface. However, different meteorological conditions in the two reanalyses used (JRA-25 and ERA-Interim) might also play a role. Note that there is an apparent artefact in the ice surface temperature in the SMOS-SIT product: it has a constant value of around -4°C for extended periods in November and December. Differences in snow thicknesses (Figure 5c) mirror differences in the ice thickness, because SMOS-SIT assumes an empirical piecewise linear relationship between the two (Tian-Kunze et al., 2014). Perhaps more importantly than all previous considerations, sensitivity studies by Maaß (2013) suggest that the decrease in TB could be the result of the sea ice becoming fresher at a different rate than assumed by the empirical rate assumed by SMOS-SIT. Testing this hypothesis is beyond the scope of this paper, because neither does SMOS-SIT deliver the assumed sea ice salinity as part of the data product, nor does the ORAS5 sea ice model have a good treatment of ice salinity. Further investigation should be undertaken, and we suggest that the assumed sea ice salinity be made part of the SMOS-SIT data product.

[Figure 5 about here.]

5 Interannual variability

Despite the uncertainties at a local scale discussed in the previous sections, there is good agreement in the large-scale distribution of thin sea ice and its interannual variability. Figure 6 shows time series of the area covered by sea ice with thickness above various thresholds in November from 2011 to 2016. the uppermost curve is the area of sea ice with at least 0.1 m thickness. The 0.1 m curve corresponds quite well to the NSIDC sea ice extent if the observational gap around the North Pole is taken into account. The lowermost curve is the area of sea ice with at least 0.9 m thickness.

There is generally good agreement between the overall magnitude, variability and trend of the area of the various thickness classes as simulated by ORAS5 and observed by SMOS. The extreme summer minimum in 2012 is visible as reduced sea ice area in November for all thickness classes. In 2013, there was a marked recovery. Since then, there has been a downward trend in all classes. Importantly, this indicates that the well-established summer sea ice decline in recent years has started to affect the winter-time state. These signals of interannual variability are in good agreement with ice volume estimates derived from CryoSat2 radar altimetry (Tilling et al., 2015).

It is important to recall that, in the thickness range 0.9 m and above, SMOS-SIT heavily relies on auxiliary fields to retrieve the sea-ice thickness from SMOS brightness temperature. To produce Figure 6 it was necessary to consider all SMOS-SIT data

points, even those with high uncertainty and/or saturation ratio close to 100%. As shown in Appendix D, the resulting maps and scatter densities are not realistic, and one should be cautious when interpreting the lowermost curve in Figure 6a. Nevertheless, it is encouraging to see that overall the same interannual variability and trends of thin sea ice area are derived from ORAS5 and SMOS-SIT.

[Figure 6 about here.]

Interannual variability and trends for sea ice in the Arctic do not occur homogeneously. Figure 6 shows November conditions, when sea ice is present not only in the central Arctic Ocean, but also in the adjacent Seas, in the Canadian Archipelago, The Baffin Bay, Labrador Sea and the Hudson Bay. All these regions are exposed to regional climate variability and change that is not necessarily aligned: the Barents, Kara and Laptev Seas are heavily influenced by the North Atlantic inflow. In the East Siberian, Chukchi and Beaufort Seas the role of the North Atlantic diminishes, and other processes related to the Siberian High and inflow Pacific climate become important.

In the East Siberian, Chukchi, and Beaufort Seas (Figure 7a,b), interannual variability of area cover is higher for thicker ice than it is for thinner ice. This feature is detected by both SMOS-SIT and ORAS5; it is more pronounced in ORAS5, where the area covered by ice thicker than 0.7 m more than doubled between 2012 and 2013, and than decreased in each subsequent to reach the same level as 2012 in 2016.

The Barents, Kara and Laptev Seas (Figure 7c,d), also exhibit a strongly reduced area coverage in 2012 for all thickness categories. However, ice cover continued to increase until 2014, by which time the area covered was almost twice as high as 2012 in some categories. The unusually high area cover in 2014 might at least in parts be due to an unusual circulation in autumn 2014: anomalously high pressure over Scandinavia combined with low pressure over Siberia in September-November led to anomalous high northerly components in the winds in these seas, which would have both encouraged thermodynamic ice growth and spreading of the ice by advection.

Another interesting feature in the Barents, Kara, and Laptev Seas is the increasing area of ice thicker than 0.9 m simulated by ORAS5. The year-to-year changes in thicker ice area as seen by SMOS-SIT are very different, but we would advise caution when interpreting the SMOS-SIT time series for these thicker ice categories for the reasons detailed in Appendix D.

Finally, in Canadian waters, the Baffin Bay, and the Labrador Sea (Figure 7e,f), no decrease in ice area for any category is detected, neither by SMOS-SIT nor by ORAS5. Relative year-to-year variations in ice area also tend to be much smaller than in the other two areas.

[Figure 7 about here.]

6 Discussion

In light of the previously discussed shortcomings and uncertainties both in the current version of the SMOS-SIT data and the current version of the ECMWF sea ice model, we suggest to proceed with caution. It is clear that there is a generic trend for

analysed sea ice to be thicker than what is retrieved from SMOS. Indications are that both problems in the model and in the observations contribute to this.

On the model side, the lack of ice thickness categories in combination with an artificial threshold of minimum ice thickness while freezing leads to overestimation of ice thicknesses during freeze-up season (October-December). Later in winter, the model is mostly incapable of simulating the polynyas and fracture zones present in the interior of the ice pack.

On the observational side, low sensitivity of the SMOS brightness temperatures for ice thicknesses larger than 0.5 m is compensated in the SMOS-SIT retrieval algorithm by heavily relying on auxiliary fields from external sources, such as 2 m temperature and winds, sea ice salinity, and snow thickness on sea ice. These have considerable and poorly quantified uncertainties associated with them, which reflects in uncertainty in the retrieved ice thickness.

The previous example illustrates that analysis-observation departures have different fundamental reasons, and future data assimilation studies using SMOS should treat each of the following scenarios differently:

1. The model over- or underestimates large-scale ice thickness in the areas of first-year ice. Typical is an overestimation in October-December in the Arctic Shelf Seas. Sea-ice thickness as derived by SMOS is within the range of the unconstrained sea-ice model, so that data assimilation will unequivocally provide a better estimate of the truth than model or observations alone.

2. SMOS-SIT systematically underestimates ice thickness. We argue that this typically occurs in the Baffin Bay and Labrador Sea during late winter. Assimilating SMOS-SIT data here would deteriorate the simulated state. We would argue that the quality of the observational product in this region needs to be improved before using it for data assimilation.

3. SMOS-SIT detects the presence of thin ice in fracture zones and polynyas, but the model has structural limitations that prevent it from simulating these. Here, SMOS-SIT can contribute to model validation and improvement. Assimilating SMOS-SIT data would lead to a better state estimate, but would force the model outside the range of states it would normally occupy. Assimilation is probably beneficial to arrive at better state estimates and initial conditions, but investigation is needed to ensure no undesired unphysical side-effects are triggered during the assimilation.

With further progress in the retrieval algorithms and the modelling for thin sea ice, the distinction between the above three departure scenario might become obsolete, and direct, unqualified use of the data for model validation and data assimilation will become possible. Until then, we suggest to use SMOS-SIT data as a means of detecting the presence of thin sea ice, and design data assimilation studies with the above three departure scenarios in mind.

7 Conclusions

It has been demonstrated here that there is huge potential for sea ice thickness from SMOS to be useful for validation of and data assimilation in prognostic ocean/sea ice models, but that there are outstanding questions on the uncertainty of the retrieved ice thickness.

Departures of ice thickness between the ice-ocean analysis ORAS5 and the SMOS-SIT observational product have a complex structure and depend on the region, season, and thickness range considered. In general, there is reasonable agreement between observed and analysed ice thickness early in the freezing season from October to November. Later on, in most regions the analysis shows ice thickness that are continuously growing, whereas SMOS ice thickness saturates. This saturation occurs even when filtering out data that is flagged as having a low uncertainty in the SMOS-SIT data product.

Some large late-winter departures are due to the occurrence of fracture zones and polynyas within the ice pack. These are well-detected by SMOS-SIT, but only poorly simulated by the model. Other late-winter departures, for instance in the Baffin Bay region, seem to be caused by SMOS-SIT data being biased low. Some hypotheses for the low bias have been suggested, but further investigation is needed here.

Despite the local uncertainties, there is good agreement in the large-scale distribution of thin sea ice, and in its interannual variability and trends. Early in the freezing season, SMOS-SIT and ORAS5 consistently show a marked depletion of thin ice in 2012, a temporary recovery in 2013/14, and a marked subsequent decrease after that, leading to a thin ice area in 2016 that is as low or lower than that in 2012.

Thin sea ice is a fast-changing moderator of air-sea heat fluxes in the cold season, with clear relevance for numerical prediction of weather and climate. However, its properties are difficult to model, and difficult to observe in-situ and remotely.

Sea-ice thickness retrievals from L-band missions like SMOS are novel and innovative, and we are only just beginning to harness its unique benefits. However, it needs to be kept in mind that this remote sensing technique is fundamentally limited to thin sea ice, and careful investigations are required to quantify this limit.

By contrasting L-Band sea-ice thickness retrievals with sea-ice thickness from an independent ocean reanalysis over seven winters 2010 to 2016, the present study explores the limits of both data sets. There is encouraging agreement in some aspects, but systematic discrepancies in other aspects. A case-by-case consideration is necessary to determine whether the truth most likely lies closer to the observational or the reanalysis data set.

In the light of these findings, we advise caution when using sea-ice thickness from SMOS for model validation and data assimilation. To make progress in reconciling observation and model data, it would be beneficial to integrate the retrieval model better with the systems that are used to produce the ancillary data for the retrieval, most importantly the meteorological and oceanographic surface parameters. This integration would allow a systematic analysis of the uncertainties and sensitivities of retrieved sea ice thickness, which in turn is an essential step towards assimilation of sea-ice thickness within a well-balanced data assimilation system. Eventually, a full exploitation of the information about sea-ice thickness contained in L-Band radiometry will lead to a better sea-ice analysis, and hence to better forecasts in polar regions from days to seasons.

Appendix A: Changes from the previous data version

In the previous data version 2.1, look-up tables were used in the retrieval algorithm to speed up processing. The resulting discretisation leads to a substantial retrieval artefact. As Figure 8 demonstrates, the frequency distribution of retrieved sea ice thickness (SIT) has an unphysical multi-mode structure, with local minima at around 15, 25, 45 and 80 cm. These modes are

very strong, for instance SMOS-SIT has four times more sea ice at 30cm than at 25cm. This artefact could potentially cause major problems in correct geophysical interpretation of the data, and could cause spurious results when using SMOS-SIT for data assimilation. In the current version 3.1 of the data, the problem has been addressed by introducing more entries in the look-up table with a finer spacing. Furthermore, in the process of converting plane-layer ice thickness into heterogeneous mean ice thickness, instead of using look-up table method, a parametrized converting function is applied, which avoid the abrupt transition caused by dividing the ice thickness into discrete entries.

[Figure 8 about here.]

Appendix B: Ambiguities when retrieving sea-ice thickness from SMOS TB

SIT retrieved from L-band microwave radiance is limited by penetration depth of the radiation in sea ice. The maximum retrievable ice thickness is reached when the L-band brightness temperature has no useful sensitivity to SIT any more, or when it is dominated by uncertain ice salinity and ice temperature (Tian-Kunze et al., 2014). Figure 9 shows that for SMOS-SIT, throughout the data set, there is a strong functional relationship between retrieved SIT and TB. TB is very sensitive to SIT of up to 50cm or so, but beyond that the slope TB/SIT of the relationship is small, meaning that SIT is only poorly constrained by TB, and auxiliary data become more important to determine the retrieved SIT.

Unfortunately, for footprints which are partially open water, SMOS-SIT does not take into account the emission of the open water. As shown in Figure 9 (middle and right), in the range 0-50cm, there is typically a sizeable open water fraction, and there is a linear relationship between ice concentration and SMOS TB. This suggest that SMOS-SIT erroneously ascribes low TB to thinner ice instead of to the open water contribution, and hence below 50cm we must expect SMOS to be biased low (see also Tian-Kunze et al. (2014)). However, this might be compensated by the fact that retrievals for sea ice concentration are often also biased low for areas of thin sea (Kwok et al., 2007). For retrieved ice thicknesses above 50cm, the open water fraction is usually low so does not contribute to the TB; however, in this range the retrieved thickness is dominated by poorly constrained assumptions about snow, ice temperature and ice salinity.

[Figure 9 about here.]

Appendix C: Day-to-day variability

Sea ice thickness at a particular location retrieved from SMOS-SIT varies much more from one day to the next than analysed by ORAS5 (Figure 10). Note that the distribution of daily SIT changes is much broader for SMOS-SIT than for ORAS5. Extreme daily thickness changes of more than 0.2 m occur around 6% of the time in SMOS-SIT, but less than 1% of the time in ORAS5. These changes can have either thermodynamic causes (ice mass changes) or advective causes (ice is moved in/out of grid cell). A SMOS-SIT grid cell has a width of 12.5km. That means, for references, an advective change of 0.2 m would require a nearby step change of 0.2 m in the ice thickness, combined with strong winds or ocean currents that are able to move the ice by 12.5 km in a day. Alternatively, if the change was thermodynamic, a surface heat flux of 700 Wm2 over that day for

the whole 12.5 km grid cell would be required. These extreme conditions should only be expected to occur near the ice edge, and in polynyas and fracture zones, and therefore daily changes of 0.2 m or more should be rare.

[Figure 10 about here.]

Inspection of maps of daily changes reveals that large SIT changes in SMOS-SIT are not restricted to the ice edge, polynyas and fracture zones, but occur over extended large-scale areas that correspond to changing synoptic weather patterns. An example is given in Figure 11. On 16 Nov 2015, ice surface temperatures derived by SMOS-SIT were around -15°C in the Laptev Sea and SMOS-derived ice thicknesses ranged between 0.5 and 1 m. The next day, SMOS-derived ice surface temperatures in this region increased by 5 K in a very coherent and homogeneous structure, while brightness temperatures decreased only slightly and with less spatial coherence. The SMOS-derived SIT over the Laptev Sea changed coherently by more than 0.2 m in some areas. Given that it is impossible for the ice to change that way in reality, taking into account both thermodynamic and advective forcing, it must be concluded that this wide-spread ice thinning by 0.2 m from one day to the next is an error in the retrieval algorithm: strong changes in the ice surface temperature, in reality caused by synoptic changes, together with unremarkable change in brightness temperatures, are erroneously interpreted as a strong thinning of the ice.

The unrealistic strong day-to-day fluctuations in the SMOS-SIT data are likely due to either errors in the ancillary fields, or due to the assumption of a linear temperature profile within the ice. If there are relevant errors in the ancillary fields, a quick change in the field will lead to a quick change in the retrieved ice thickness that is not realistic. The limits to the validity of the assumption of a linear temperature profile has been investigated in detail by Maaß (2013). They found that, after abrupt changes in the meteorological conditions, the temperature profile within the ice can take several days to adjust. Based on these results, we tentatively suggest that the assumption of the linear temperature profile within the ice is responsible for the unrealistic day-to-day changes in the SMOS-SIT data.

However, this question can only be answered satisfyingly by further research which has full control both over the SMOS-SIT retrieval model and the ancillary meteorological and oceanographic fields. At production, these ancillary fields form part of an data assimilation system, and therefore advanced and well-studied uncertainty estimates are available. It would be a valuable first step towards assimilation of SMOS brightness temperatures for SIT, if the SMOS-SIT retrieval model could be installed at one of the operational centres who produces the ancillary fields, and test sensitivity of the retrieved SIT to their known uncertainties.

[Figure 11 about here.]

Appendix D: Representation of thicker ice

When interpreting sea-ice thicknesses of 0.5 m or higher from SMOS-SIT, it is essential to inspect the provided uncertainties. Neglecting to do so easily results in wrong conclusions. As an example, Figure 12 shows sea-ice thickness on a single day (15 Nov 2012) as seen by SMOS-SIT and ORAS5. When considering all data from SMOS-SIT (Figure 12a), a false impression of almost uniformly 1 m thick sea ice throughout the Arctic Ocean is given, which is unrealistic given the well-known fact that the

multi-year ice north of Greenland and the Canadian Archipelago is several meters thick, whereas the newly formed first-year ice in the marginal seas of the Arctic Ocean is probably thinner than 1 m. Sea-ice thickness in ORAS5 (Figure 12b) clearly shows the expected structure, in good agreement with other observations and modelling results (Kwok and Cunningham, 2008; Schweiger et al., 2011; Laxon et al., 2013).

Figure 12c shows the corresponding scatter density between SMOS-SIT and ORAS5 sea ice thickness for the freeze-up season 15 Oct - 15 Dec 2012. It is evident that SMOS-SIT, without any filtering, has lots of ice thickness in the 1-1.5 m range, which do not correlate at all with the ORAS5 ice thickness.

[Figure 12 about here.]

Acknowledgements. This work was partly supported by ESA under the contract 4000101703/10/NL/FF/fk. We thank Nina Maaß, Matthias Drusch, Leif T. Pederson, and Nick Hughes for helpful discussions.

References

Daget, N., Weaver, A. T., and Balmaseda, M. A.: An ensemble three-dimensional variational data assimilation system for the global ocean: Sensitivity to the observation and background-error variance formulation, ECMWF Technical Memorandum, 562, 2008.

Dee, D. P., Uppala, S. M., Simmons, A. J., Berrisford, P., Poli, P., Kobayashi, S., Andrae, U., Balmaseda, M. A., Balsamo, G., Bauer, P., Bechtold, P., Beljaars, A. C. M., van de Berg, L., Bidlot, J., Bormann, N., Delsol, C., Dragani, R., Fuentes, M., Geer, A. J., Haimberger, L., Healy, S. B., Hersbach, H., Hólm, E. V., Isaksen, L., Kållberg, P., Köhler, M., Matricardi, M., McNally, A. P., Monge-Sanz, B. M., Morcrette, J.-J., Park, B.-K., Peubey, C., de Rosnay, P., Tavolato, C., Thépaut, J.-N., and Vitart, F.: The ERA-Interim reanalysis: configuration and performance of the data assimilation system, Quarterly Journal of the Royal Meteorological Society, 137, 553–597, doi:10.1002/qj.828, http://doi.wiley.com/10.1002/qj.828, 2011.

Donlon, C. J., Martin, M., Stark, J., Roberts-Jones, J., Fiedler, E., and Wimmer, W.: The Operational Sea Surface Temperature and Sea Ice Analysis (OSTIA) system, Remote Sensing of Environment, 116, 140–158, doi:10.1016/j.rse.2010.10.017, http://www.sciencedirect.com/science/article/pii/S0034425711002197, 2012.

Fichefet, T. and Maqueda, M. A. M.: Sensitivity of a global sea ice model to the treatment of ice thermodynamics and dynamics, Journal of Geophysical Research, 102, 12 609–12 646, doi:10.1029/97JC00480, http://doi.wiley.com/10.1029/97JC00480, 1997.

Hibler III, W. D.: A Dynamic Thermodynamic Sea Ice Model, J. Phys. Oceanogr., 9, 815–846, 1979.

Kaleschke, L., Maaß, N., Haas, C., Hendricks, S., Heygster, G., and Tonboe, R. T.: A sea-ice thickness retrieval model for 1.4 GHz radiometry and application to airborne measurements over low salinity sea-ice, Cryosphere, 4, 583–592, doi:10.5194/tc-4-583-2010, http://www.the-cryosphere.net/4/583/2010/tc-4-583-2010.html, 2010.

Kaleschke, L., Tian-Kunze, X., Maaß, N., Mäkynen, M., and Drusch, M.: Sea ice thickness retrieval from SMOS brightness temperatures during the Arctic freeze-up period, Geophysical Research Letters, 39, L05 501, doi:10.1029/2012GL050916, http://doi.wiley.com/10.1029/2012GL050916, 2012.

Kaleschke, L., Tian-Kunze, X., Maaß, N., Beitsch, A., Wernecke, A., Miernecki, M., Müller, G., Fock, B. H., Gierisch, A. M., Schlünzen, K. H., Pohlmann, T., Dobrynin, M., Hendricks, S., Asseng, J., Gerdes, R., Jochmann, P., Reimer, N., Holfort, J., Melsheimer, C., Heygster, G., Spreen, G., Gerland, S., King, J., Skou, N., Søbjærg, S. S., Haas, C., Richter, F., and Casal, T.: SMOS sea ice product: Operational application and validation in the Barents Sea marginal ice zone, Remote Sensing of Environment, 180, 264–273, doi:10.1016/j.rse.2016.03.009, 2016.

Kwok, R. and Cunningham, G. F.: ICESat over Arctic sea ice: Estimation of snow depth and ice thickness, Journal of Geophysical Research, 113, C08 010, doi:10.1029/2008JC004753, http://doi.wiley.com/10.1029/2008JC004753, 2008.

Kwok, R., Comiso, J. C., Martin, S., and Drucker, R.: Ross Sea polynyas: Response of ice concentration retrievals to large areas of thin ice, Journal of Geophysical Research, 112, C12 012, doi:10.1029/2006JC003967, http://doi.wiley.com/10.1029/2006JC003967, 2007.

Landy, J. C., Ehn, J. K., Babb, D. G., Theriault, N., and Barber, D. G.: Sea ice thickness in the Eastern Canadian Arctic: Hudson Bay Complex & Baffin Bay, Remote Sensing of Environment, 200, 281–294, doi:10.1016/J.RSE.2017.08.019, http://www.sciencedirect.com/science/article/pii/S0034425717303887?via{%}3Dihub, 2017.

Laxon, S. W., Giles, K. A., Ridout, A. L., Wingham, D. J., Willatt, R., Cullen, R., Kwok, R., Schweiger, A., Zhang, J., Haas, C., Hendricks, S., Krishfield, R., Kurtz, N., Farrell, S., and Davidson, M.: CryoSat-2 estimates of Arctic sea ice thickness and volume, Geophysical Research Letters, 40, 732–737, doi:10.1002/grl.50193, http://doi.wiley.com/10.1002/grl.50193, 2013.

Maaß, N.: Remote sensing of sea ice thickness using SMOS data, Ph.D. thesis, University of Hamburg, 2013.

Madec, G.: NEMO ocean engine, Tech. rep., Institut Pierre-Simon Laplace (IPSL), http://www.nemo-ocean.eu/About-NEMO/Reference-manuals, 2008.

Mäkynen, M., Cheng, B., and Similä, M.: On the accuracy of thin-ice thickness retrieval using MODIS thermal imagery over Arctic first-year ice, Annals of Glaciology, 54, 87–96, doi:10.3189/2013AoG62A166, https://www.cambridge.org/core/product/identifier/S0260305500260266/type/journal{_}article, 2013.

Marshall, J., Adcroft, A., Hill, C., Perelman, L., and Heisey, C.: A finite-volume, incompressible Navier Stokes model for studies of the ocean on parallel computers, Journal of Geophysical Research: Oceans, 102, 5753–5766, doi:10.1029/96JC02775, http://doi.wiley.com/10.1029/96JC02775, 1997.

Mecklenburg, S., Drusch, M., Kaleschke, L., Rodriguez-Fernandez, N., Reul, N., Kerr, Y., Font, J., Martin-Neira, M., Oliva, R., Daganzo-Eusebio, E., Grant, J., Sabia, R., Macelloni, G., Rautiainen, K., Fauste, J., de Rosnay, P., Munoz-Sabater, J., Verhoest, N., Lievens, H., Delwart, S., Crapolicchio, R., de la Fuente, A., and Kornberg, M.: ESA's Soil Moisture and Ocean Salinity mission: From science to operational applications, Remote Sensing of Environment, 180, 3–18, doi:10.1016/j.rse.2015.12.025, 2016.

Menashi, J. D., St. Germain, K. M., Swift, C. T., Comiso, J. C., and Lohanick, A. W.: Low-frequency passive-microwave observations of sea ice in the Weddell Sea, Journal of Geophysical Research, 98, 22 569, doi:10.1029/93JC02058, http://doi.wiley.com/10.1029/93JC02058, 1993.

ONOGI, K., TSUTSUI, J., KOIDE, H., SAKAMOTO, M., KOBAYASHI, S., HATSUSHIKA, H., MATSUMOTO, T., YAMAZAKI, N., KAMAHORI, H., TAKAHASHI, K., KADOKURA, S., WADA, K., KATO, K., OYAMA, R., OSE, T., MANNOJI, N., and TAIRA, R.: The JRA-25 Reanalysis, Journal of the Meteorological Society of Japan. Ser. II, 85, 369–432, doi:10.2151/jmsj.85.369, https://www.jstage.jst.go.jp/article/jmsj/85/3/85{_}3{_}369/{_}article, 2007.

Ricker, R., Hendricks, S., Helm, V., Skourup, H., and Davidson, M.: Sensitivity of CryoSat-2 Arctic sea-ice freeboard and thickness on radar-waveform interpretation, The Cryosphere, 8, 1607–1622, doi:10.5194/tc-8-1607-2014, http://www.the-cryosphere.net/8/1607/2014/tc-8-1607-2014.html, 2014.

Schweiger, A., Lindsay, R., Zhang, J. L., Steele, M., Stern, H., and Kwok, R.: Uncertainty in modeled Arctic sea ice volume, J. Geophys. Res., 116, C00D06, doi:10.1029/2011JC007084, 2011.

Semtner, A. J.: A Model for the Thermodynamic Growth of Sea Ice in Numerical Investigations of Climate, J. Phys. Oceanogr., 6, 379–389, 1976.

Tian-Kunze, X., Kaleschke, L., Maaß, N., Mäkynen, M., Serra, N., Drusch, M., and Krumpen, T.: SMOS-derived thin sea ice thickness: algorithm baseline, product specifications and initial verification, The Cryosphere, 8, 997–1018, doi:10.5194/tc-8-997-2014, http://www.the-cryosphere.net/8/997/2014/tc-8-997-2014.html, 2014.

Tietsche, S., Notz, D., Jungclaus, J. H., and Marotzke, J.: Assimilation of sea-ice concentration in a global climate model – physical and statistical aspects, Ocean Science, 9, 19–36, doi:10.5194/os-9-19-2013, http://www.ocean-sci.net/9/19/2013/os-9-19-2013.html, 2013.

Tietsche, S., Balmaseda, M. A., Zuo, H., and Mogensen, K.: Arctic sea ice in the ECMWF MyOcean2 ocean reanalysis ORAP5, Tech. Rep. 737, European Center for Medium-Range Weather Forecasts, Reading, UK, http://old.ecmwf.int/publications/library/ecpublications/{_}pdf/tm/701-800/tm737.pdf, 2014.

Tietsche, S., Balmaseda, M. a., Zuo, H., and Mogensen, K.: Arctic sea ice in the global eddy-permitting ocean reanalysis ORAP5, Climate Dynamics, doi:10.1007/s00382-015-2673-3, http://link.springer.com/10.1007/s00382-015-2673-3, 2015.

Tilling, R. L., Ridout, A., Shepherd, A., and Wingham, D. J.: Increased Arctic sea ice volume after anomalously low melting in 2013, Nature Geoscience, advance on, doi:10.1038/ngeo2489, http://dx.doi.org/10.1038/ngeo2489, 2015.

Wang, X., Key, J. R., and Liu, Y.: A thermodynamic model for estimating sea and lake ice thickness with optical satellite data, Journal of Geophysical Research, 115, C12 035, doi:10.1029/2009JC005857, http://doi.wiley.com/10.1029/2009JC005857, 2010.

Yu, Y. and Rothrock, D. A.: Thin ice thickness from satellite thermal imagery, Journal of Geophysical Research: Oceans, 101, 25 753–25 766, doi:10.1029/96JC02242, http://doi.wiley.com/10.1029/96JC02242, 1996.

Zuo, H., Balmaseda, M. A., and Mogensen, K.: The new eddy-permitting ORAP5 ocean reanalysis: description, evaluation and uncertainties in climate signals, Climate Dynamics, doi:10.1007/s00382-015-2675-1, http://link.springer.com/article/10.1007{%}2Fs00382-015-2675-1, 2015.

Zuo, H., Balmaseda, M. A., Boisseson, E., and Hirahara, S.: A new ensemble generation scheme for ocean reanalysis, ECMWF Technical Memorandum, 795, 2017.

The Cryosphere Discuss., https://doi.org/10.5194/tc-2017-247
Manuscript under review for journal The Cryosphere
Discussion started: 1 December 2017

List of Figures

The Cryosphere Discuss., https://doi.org/10.5194/tc-2017-247
Manuscript under review for journal The Cryosphere
Discussion started: 1 December 2017

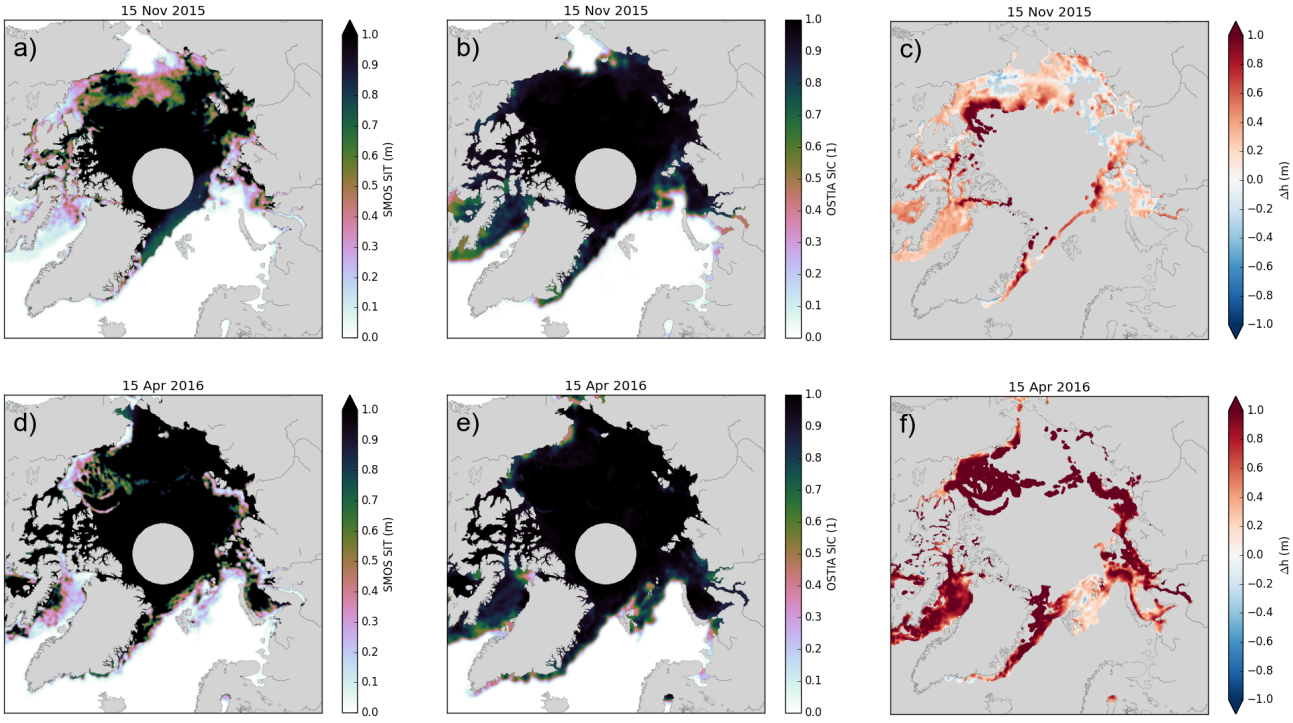

Figure 1. Thin sea ice for two selected days representing typical conditions in early and late winter: 15 Nov 2015 (a)–(c) and 15 April 2016 (d)–(f). Subfigures (a) and (d) show the sea ice thickness retrieved by SMOS-SIT. The colours saturate at 1m, because ice thicknesses beyond that can normally not be retrieved. Subfigures (b) and (e) show sea ice concentration from the OSTIA product. The difference between sea ice thickness analyzed in ORAS5 and retrieved by SMOS-SIT is shown in (c) and (f). For the difference, SMOS-SIT grid cells with saturation ratio larger than 90% or an estimated retrieval uncertainty of $>$ 1m have been excluded.

The Cryosphere Discuss., https://doi.org/10.5194/tc-2017-247
Manuscript under review for journal The Cryosphere
Discussion started: 1 December 2017

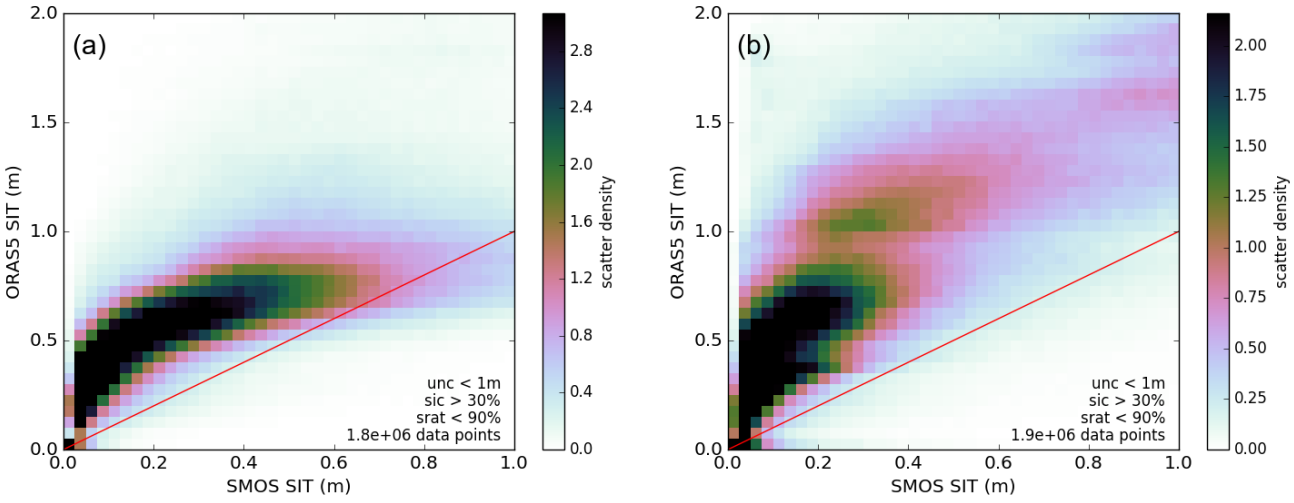

Figure 2. Scatter density of observed and analysed thin sea ice, (a) October to December 2015, (b) February to April 2016.

The Cryosphere Discuss., https://doi.org/10.5194/tc-2017-247
Manuscript under review for journal The Cryosphere
Discussion started: 1 December 2017

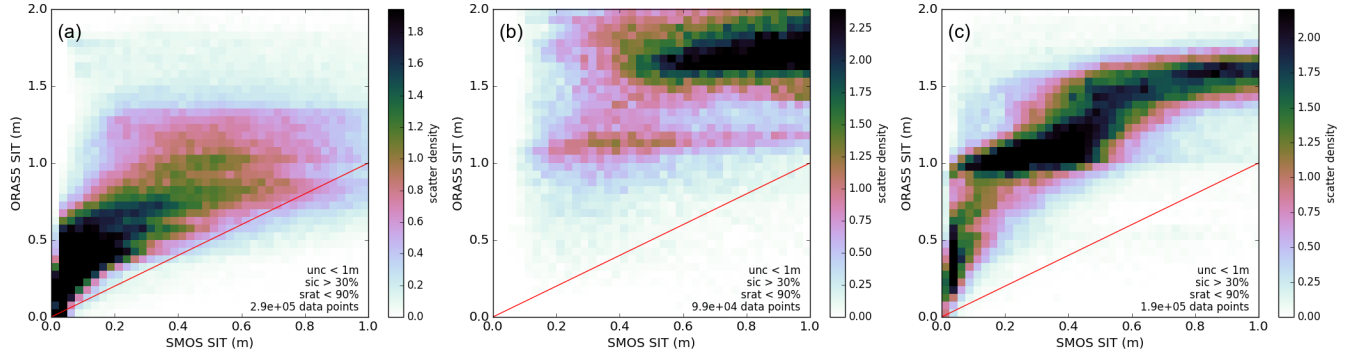

Figure 3. Scatter density of observed and analysed thin sea ice in late winter, February to April 2016: (a) Barents and Kara Seas (15E–90E, 70–85N), (b) Laptev Sea (90E–150E, 70–85N), and (c) Baffin Bay (75W–53W, 65N–80N).

The Cryosphere Discuss., https://doi.org/10.5194/tc-2017-247
Manuscript under review for journal The Cryosphere
Discussion started: 1 December 2017

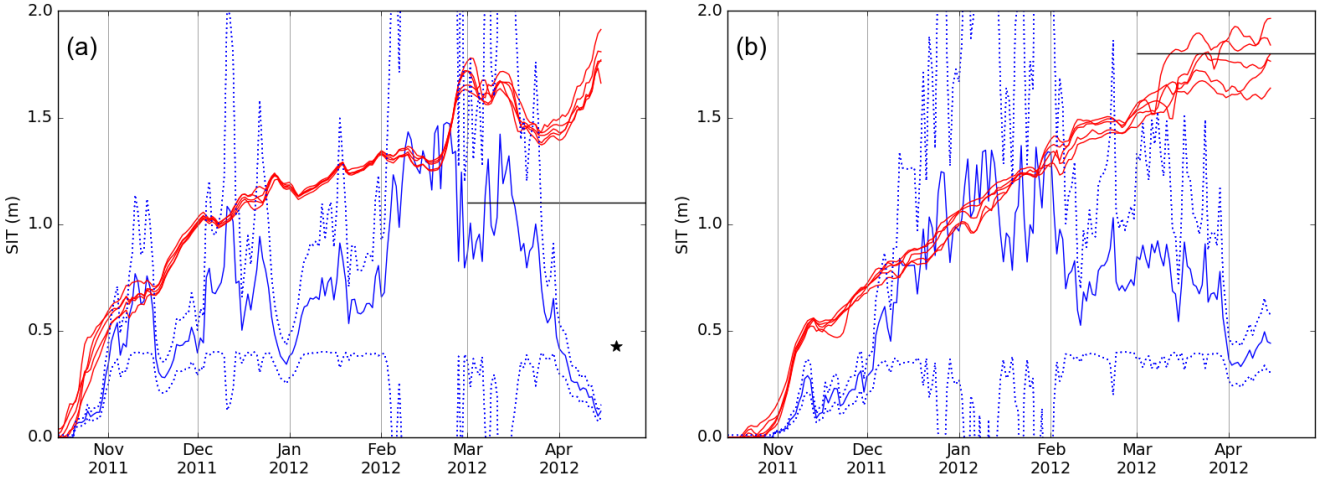

Figure 4. Time series of daily sea ice thickness during the 2011/2012 winter at (a) a representative location in the Laptev Sea at 74.5N,127E and (b) a representative location in the Baffin Bay at 72N,62W. Blue is SMOS-SIT (full line) with added and subtracted (dotted lines); Red are the five realisations of ORAS5; Black horizontal lines are the CryoSat2 average thickness for March/April provided by CPOM; black star is an EM-Bird overfly for the Laptev Sea on 20 April 2012.

The Cryosphere Discuss., https://doi.org/10.5194/tc-2017-247
Manuscript under review for journal The Cryosphere
Discussion started: 1 December 2017

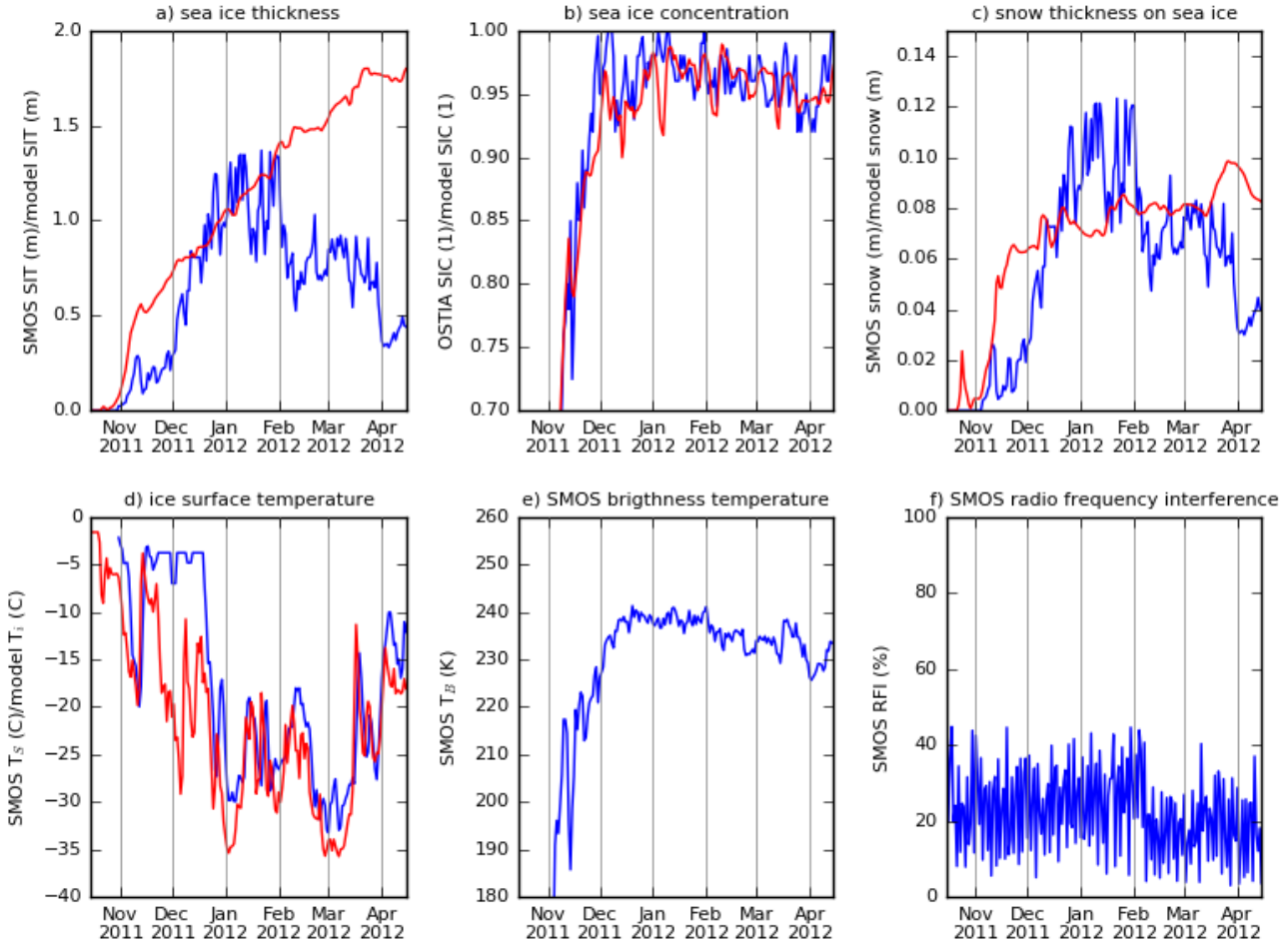

Figure 5. Time series for relevant SMOS-SIT and ORAS5 parameters for the Baffin Bay location 72N,72W for the full freezing season 2011/2012. Blue curves are SMOS-SIT parameters (except in (b), where blue is observed ice concentration from OSTIA), red curves are model parameters.

The Cryosphere Discuss., https://doi.org/10.5194/tc-2017-247
Manuscript under review for journal The Cryosphere
Discussion started: 1 December 2017

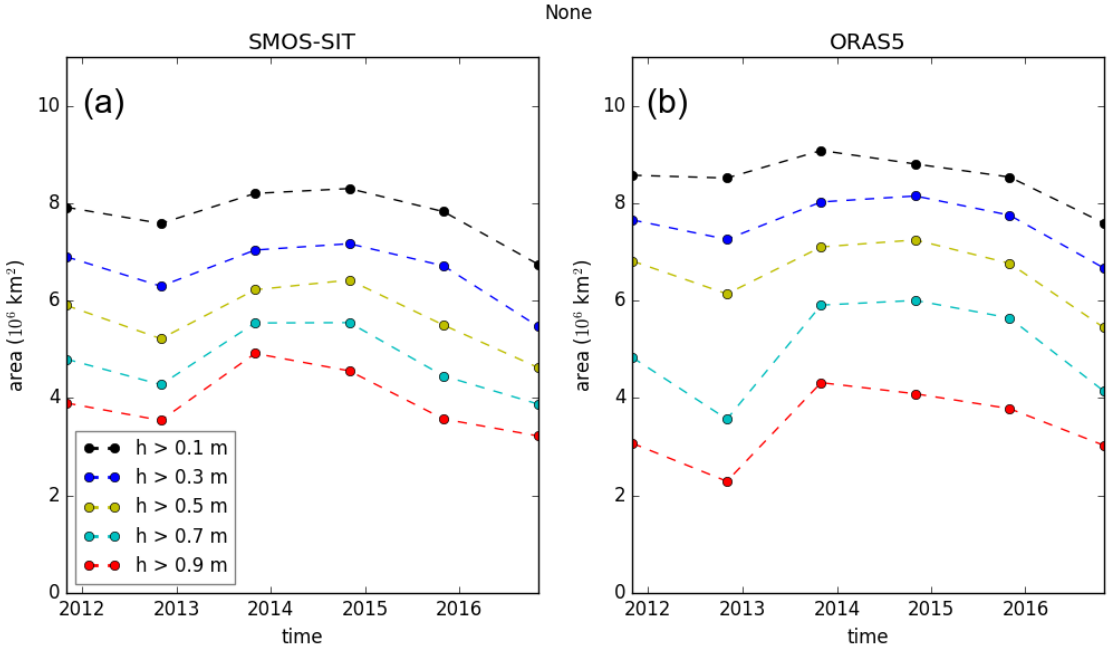

Figure 6. Monthly November means of the pan-Arctic area covered by ice thicker than given thresholds in SMOS-SIT (a) and ORAS5 (b).

The Cryosphere Discuss., https://doi.org/10.5194/tc-2017-247
Manuscript under review for journal The Cryosphere
Discussion started: 1 December 2017

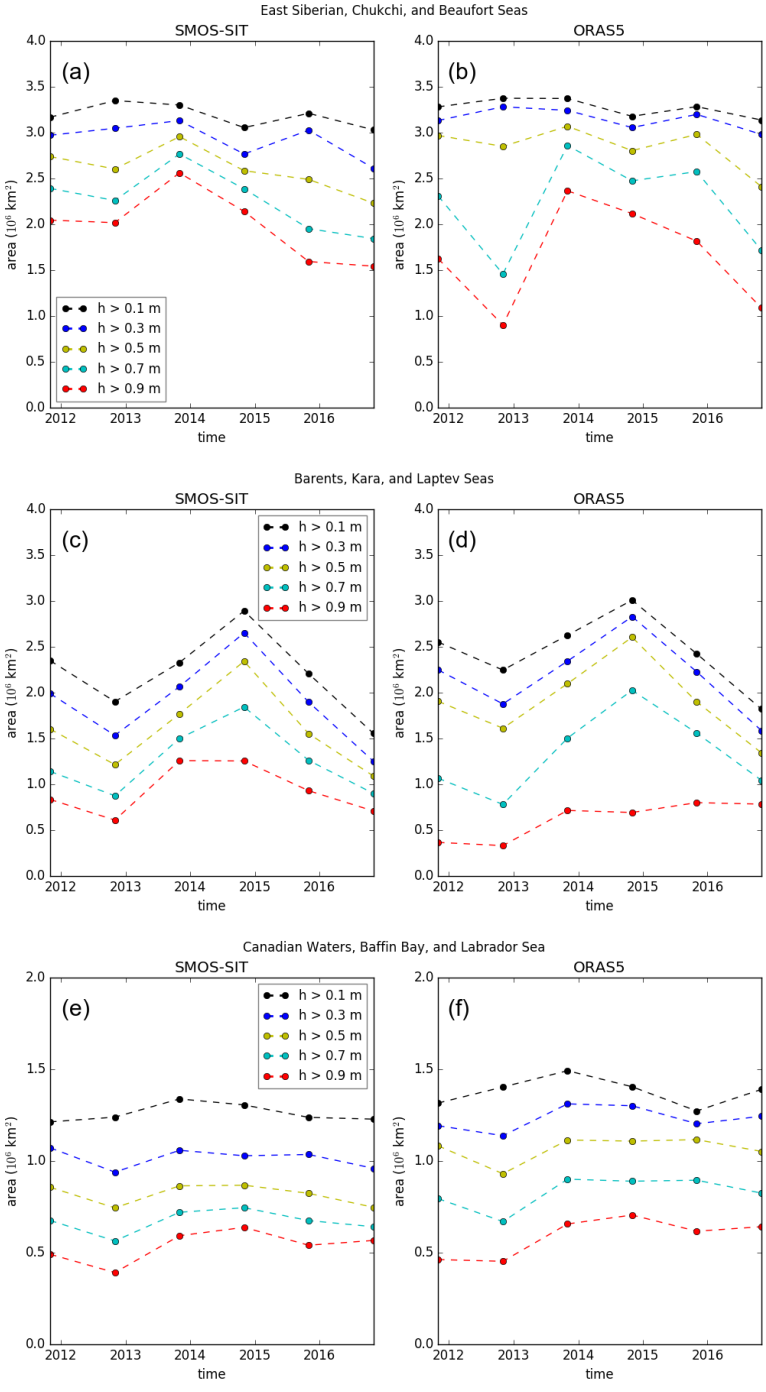

Figure 7. Monthly November means of the regional area covered by ice thicker than given thresholds in SMOS-SIT (left) and ORAS5 (right). The boundaries of the longitude-latitude boxes are 0-150E, 70-90N for (a) and (b); 150E-120W, 70-90N for (c) and (d); and 120-70W, 55-83N for (e) and (f).

The Cryosphere Discuss., https://doi.org/10.5194/tc-2017-247
Manuscript under review for journal The Cryosphere
Discussion started: 1 December 2017

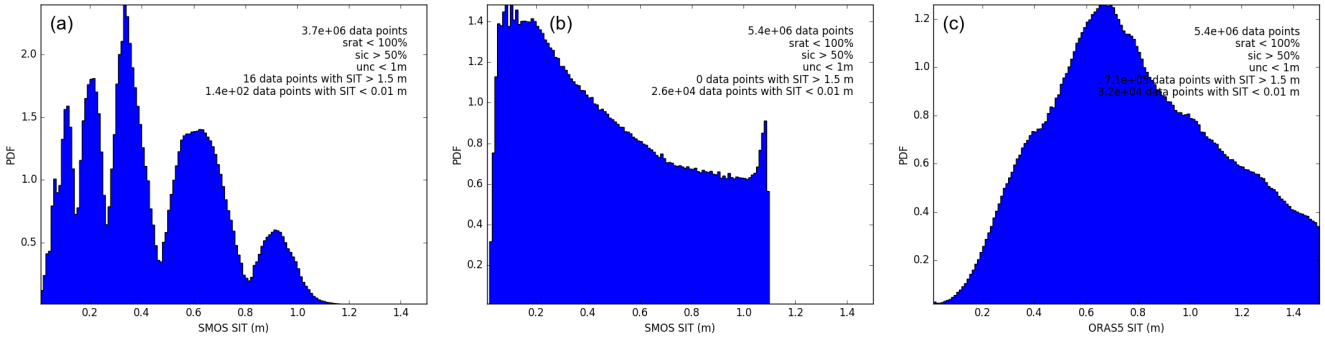

Figure 8. SMOS-SIT thickness frequency distribution for the winter 2015/2016 for SMOS-SIT version 2.1 (left), SMOS-SIT version 3.1 (middle), and the ORAS5 ocean/sea ice reanalysis (right).

The Cryosphere Discuss., https://doi.org/10.5194/tc-2017-247
Manuscript under review for journal The Cryosphere
Discussion started: 1 December 2017

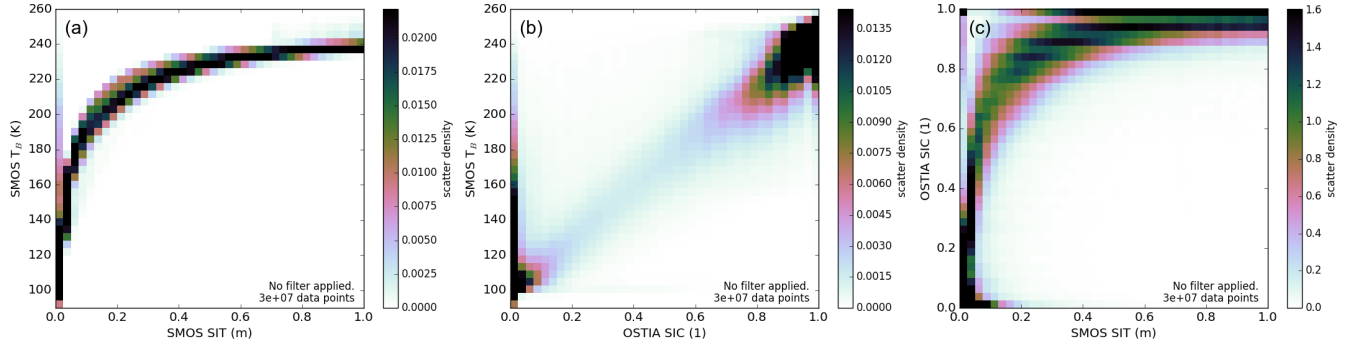

Figure 9. Scatter density of (a) SMOS TB and SMOS-SIT-derived sea ice thickness, (b) SMOS TB and sea-ice concentration, (c) sea-ice concentration and SMOS-SIT sea-ice thickness. The scatter density is calculated from all SMOS-SIT data points over the period 15 Oct 2015 to 15 Apr 2016, no filtering has been applied.

The Cryosphere Discuss., https://doi.org/10.5194/tc-2017-247
Manuscript under review for journal The Cryosphere
Discussion started: 1 December 2017

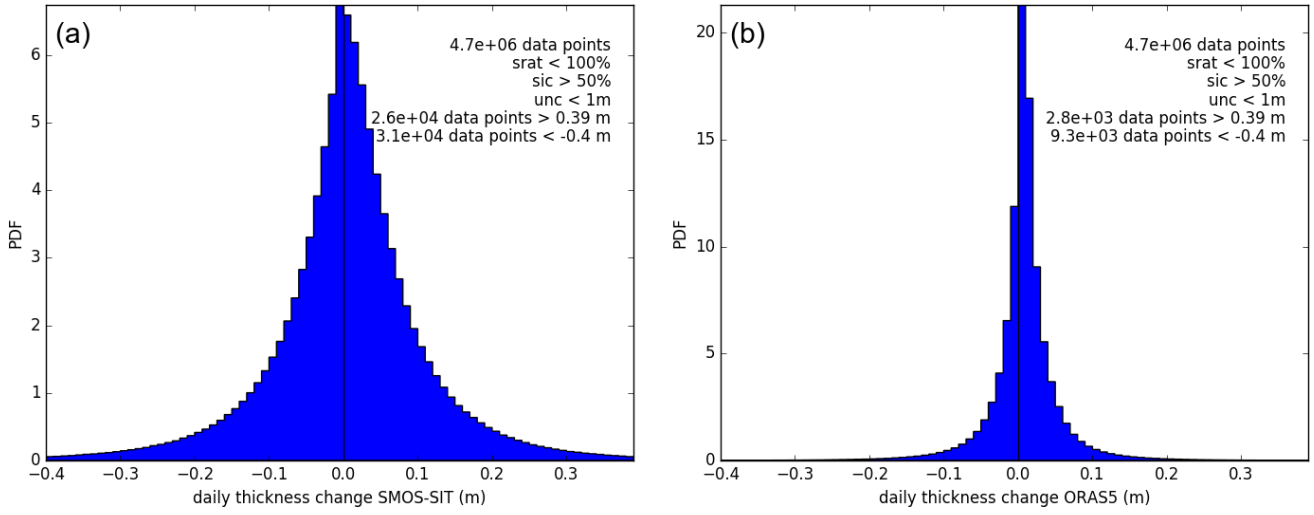

Figure 10. Frequency distribution of SMOS-SIT-derived (left) and ORAS5 (right) daily sea ice thickness changes in the period 15 Oct 2015 to 15 Apr 2016. To produce these histograms, only those differences between consecutive days at the same location have been taken into account where the uncertainty diagnostics provided with SMOS-SIT for both days indicate a reliable retrieval (saturation ration $< 100\%$, uncertainty < 1 m, sea-ice concentration $> 50\%$). Day-to-day thickness changes are outside ± 0.4 m in less than 1% of the cases.

The Cryosphere Discuss., https://doi.org/10.5194/tc-2017-247
Manuscript under review for journal The Cryosphere
Discussion started: 1 December 2017

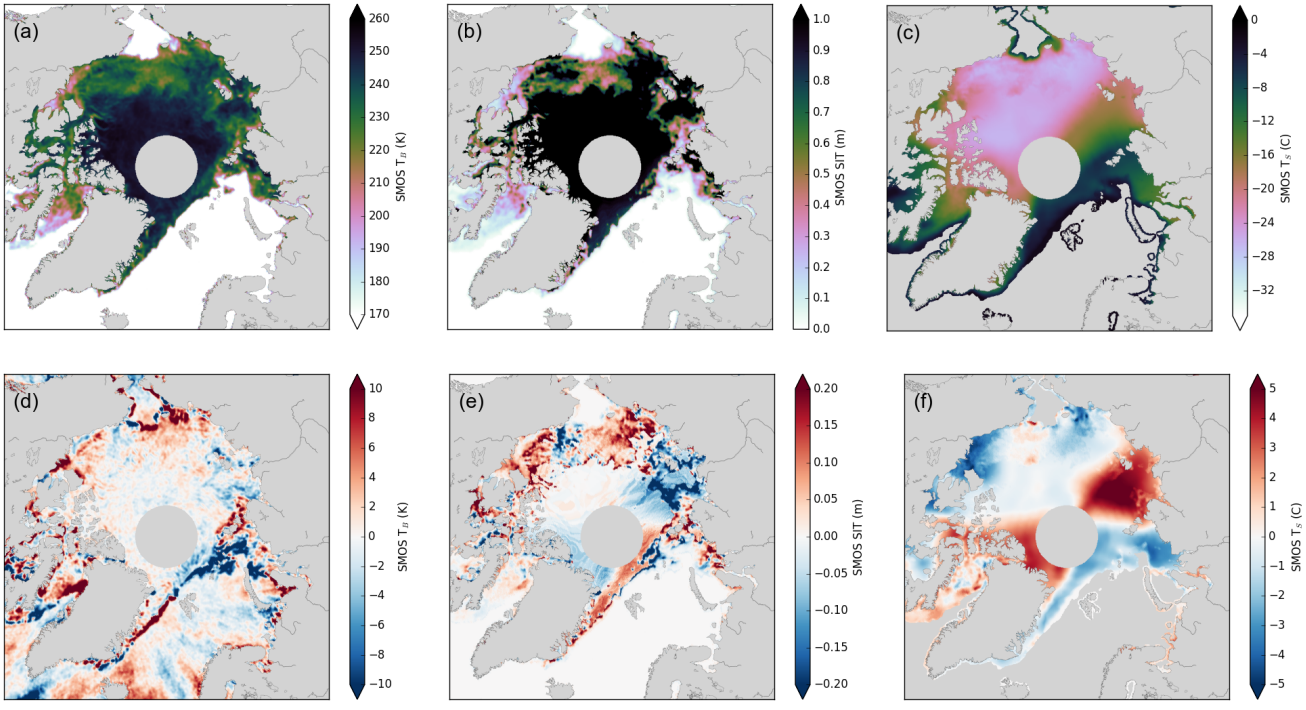

Figure 11. SMOS-derived information on 15 November 2015 (top panels) and daily difference between 16 and 15 November 2015 (bottom panels) for SMOS TB (a,d), SMOS-SIT ice thickness (b,e) and SMOS-SIT ice surface temperature (c,f). Correspondence between unrealistic SMOS-derived changes in ice thickness (e) and changes in ice surface temperatures (d) are evident.

The Cryosphere Discuss., https://doi.org/10.5194/tc-2017-247
Manuscript under review for journal The Cryosphere
Discussion started: 1 December 2017

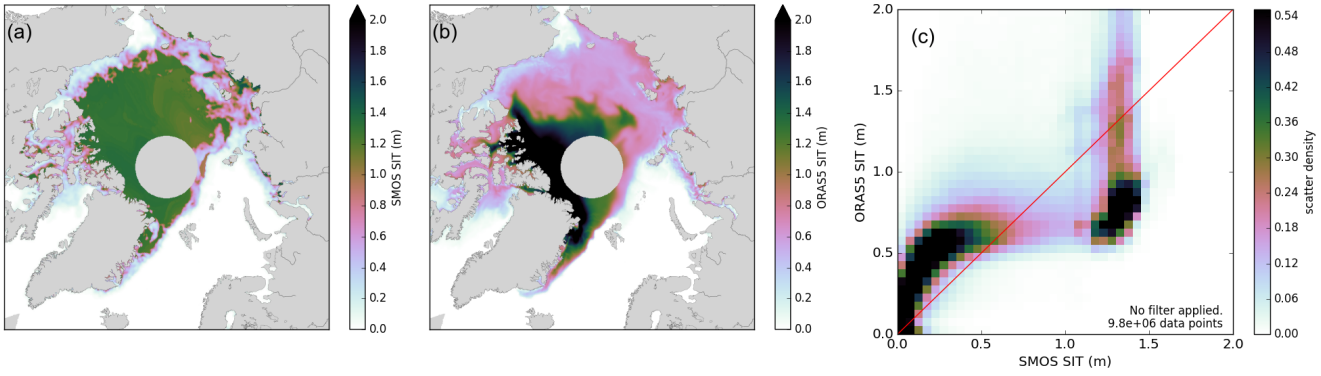

Figure 12. Representation of thicker ice in SMOS-SIT and ORAS5. (a) and (b) show sea-ice thickness on 15 Nov 2012 in the range 0-2 m derived from (a) SMOS-SIT and (b) ORAS5. (c) shows the scatter density of ice thickness from SMOS-SIT and ORAS5 for all observation points without any filtering from 15 Oct to 15 Dec 2012.